Manganese Constituent in Stainless Steels Oxidized in Oxygen Containing Water Vapor at 800 ºC: High Temperature Oxidation and Volatilization

Methanan Sangsuebsri[1], *Suwijak* Pokwitidkul[1], *Panya* Wiman[1], *Youhei* Tanaka[2] and *Thammaporn* Thublaor[1,*]

[1]High Temperature Corrosion Research Centre, Department of Materials and Production Technology Engineering, Faculty of Engineering, King Mongkut's University of Technology North Bangkok, 1518, Pracharat 1 Road, Bangsue, Bangkok 10800, Thailand
[2]Division of Materials Science and Engineering, Graduate School of Engineering, Muroran Institute of Technology, 27-1 Mizumoto, Muroran 0508585, Japan

Abstract. Many industrial operations, such as solid oxide fuel cells (SOFCs) or combustion processes, have water vapor environments. Stainless steel was applied as part of these applications at high temperatures. The present work investigates high and low manganese content stainless steel that oxidized in an oxygen-containing 5% water vapor at 800 ºC. SEM and EDX were performed to analyze oxide formation and ICP-OES was used to detect the volatile species that evaporated from steel surfaces. The results show that manganese in steel increases spallation and reduces Cr volatilization rates in high Mn stainless steel. The average Cr volatilization of high Mn samples is 0.09×10^{-11} g cm^{-2} s^{-1}, which is about 14 times lower than the ones (1.25×10^{-11} g cm^{-2} s^{-1}), while Fe and Mn volatilization rates increase by 10 and 62 times, respectively.

Keyword. High temperature oxidation, Manganese content, Volatilization, Water vapor

1 Introduction

Stainless steel has been extensively used in various industrial applications. This is due to their excellent oxidation resistance and good mechanical properties. Chromium oxide (Cr_2O_3) can form on stainless steel which has a high chromium content (> 10.5-12.0 wt.%) [1]. It provides a dense, continuous, adherent steel substrate and a relatively slow growth rate. The prevention of Cr_2O_3 helps to increase high-temperature corrosion resistance and reduce the maintenance process due to material loss. Stainless steel is substantially more corrosive in the atmosphere containing water vapor than dry air [2,3], and this often arises in many applications. It has been reported that the amount of water vapor important to the hot-rolling process is around 19.5% [4] and can reach up to 40.0% in the combustion process [5]. Including solid oxide fuel cells (SOFCs), which are potential technologies for producing sustainable energy [6]. The water vapor can induce Cr evaporation from the chromium oxide in the form of $CrO_2(OH)_{2(g)}$ at lower temperatures of 1500 ºC, as follows: (1) [7].

$$\frac{1}{2}Cr_2O_{3(g)} + \frac{3}{4}O_{2(g)} + H_2O_{(g)} \rightarrow CrO_2(OH)_{2(g)} \quad (1)$$

As a result of chromia evaporation and inadequate Cr supplied from the steel, the protective Cr-rich oxide transforms into a non-protective Fe-rich oxide, and breakaway oxidation ensues [8]. Besides chromium in stainless steel, manganese is a common constituent element in alloys and affects oxidation resistance. When high content is added to alloys, it can create an austenite phase, which is regarded as a nickel substitute for the production of austenitic stainless steel grades [9,10]. It also is seven times cheaper than nickel at an equivalent weight [11,12]. Indeed, various studies have been conducted on the effect of low-level manganese additions on the oxidation resistance of (Fe, Ni, or Co)-Cr alloys since 1970. The scales created were proportional to the bulk chromium content [13-15]. They observed that adding up to 5% manganese to alloys containing around 20% chromium resulted in the creation of $MnCr_2O_4$.

For SOFCs with metallic interconnects, H. Falk-Windisch *et. al.,* [16] studied Sanergy HT (0.25 wt.%Mn) and Crofer 22 H (0.40 wt.%Mn) stainless steels of chromium content ~23 wt.% in air-3% H_2O at 650, 750 and 850 ºC. They found that the presence of manganese in steels at high temperatures with low content contributes to the formation of a duplex-layered oxide scale with an outer layer of $(Mn, Cr)_3O_4$ whereas Cr_2O_3 is underneath. Moreover, the mass gain of Crofer 22 H stainless steel was higher than the others but reduced in chromium volatilization. This is due to the effect of Mn on the production of a continuous top layer of $(Cr,Mn)_3O_4$, which decreases Cr activity at the metal substrate compared to Cr_2O_3. Despite the fact that prior research [13-16] continues to examine the impact of manganese in alloys on oxidation resistance at high temperatures. These studies still lack an investigation of

* Corresponding author: thammaporn.t@eng.kmutnb.ac.th

the volatilized phase that causes mass loss from steel substrates. To better understand, the effect of manganese on chromium volatilization and oxidation resistance was comparable. In the present work, stainless steel with high manganese (Fe-15.3 wt.%Cr-8.9 wt.%Mn) and low content as AISI 430 stainless steel (Fe-16.4 wt.%Cr-0.8 wt.%Mn) were studied. The samples were oxidized in an oxygen atmosphere containing water vapor at 800 °C and then collected chromium, manganese, and iron from volatile species. The oxidation mechanism of the alloy is also discussed through the dependence of manganese content on the alloy.

2 Experimental procedures

2.1 Material

An AISI 430 stainless steel (low Mn) and special grade (high Mn) were cut into rectangular shapes (15 x 15 x 1 mm^3) and its chemical composition was measured using optical emission spectroscopy (Thermo Electron Corporation, ARL 3460) and reported in Table 1. The sample was ground on silicon abrasive papers of 180 up to 1000 grits and cleaned with deionized water and ethanol in an ultrasonic bath, respectively. It was dried by an air dryer.

Table 1. Chemical composition of the studied high and low Mn stainless steel in wt.%.

Element in wt%	Stainless steel	
	Low Mn	High Mn
Cr	16.41	15.32
Mn	0.79	8.94
Si	0.20	0.45
C	0.10	0.12
Ni	0.05	0.90
P	0.03	0.07
Fe	Bal.	Bal.

2.2 Experimental setup

To begin, suspend each specimen one at a time inside a controlled-atmosphere furnace in a vertical direction, as the hottest part of the furnace is in the center. The desired furnace temperature was set at 800 °C for the test and the oxidation times were set at 1, 24, 48, 72, and 96 h. The velocity of argon gas was 1.0 cm s^{-1}. It flowed directly through the specimen in the vertical furnace while waiting for the temperature inside the furnace to rise to 800 °C. When the temperature reaches 800 °C, the oxygen gas is switched from argon with a velocity flow rate at 1.0 cm s^{-1} into a water flask. A 5% H_2O content was controlled by maintaining the water temperature at 31 °C. The temperature was calculated according to the Clausius-Clapeyron equation using the enthalpy of water vaporization, 40,893 J mol^{-1} [17]. The humidified oxygen flowed through the sample surfaces and condensed at the bottom column of the furnace. This condensate was known as a concentration solution. The tube and condenser were cleaned with 0.1 M HCl, and the cleaning solution was added to the concentration solution, which was then used to analyze the number of elements from vaporization using inductively coupled plasma optical emission spectroscopy (ICP-OES). Before and after each test, the samples were weighed using a precision balance.

2.3 Characterization

Scanning electron microscopy (SEM) was performed to provide the surface image of the sample, and SEM equipped with energy-dispersive X-ray spectroscopy (EDS) was used to examine elements. The X-ray diffraction (XRD) technique was utilized at room temperature to characterize the phases present on oxidized stainless steels, and the incident Cu-Kα, α = 1.5406 Å was utilized. XRD patterns obtained from the experiment were matched with the standard patterns by X'Pert HighScore program which was reported as an ICDD number.

3 Results and discussion

The results of the testing were reported in four sections. Firstly, oxidation was tested of both low and high Mn stainless steel oxidized in O_2-5%H_2O for 1 h up to 96 h at 800 °C. Second, the volatilization rates of the samples were measured in O_2-5%H_2O at 800 °C for 96 h. SEM-EDS results of the oxidized sample and the XRD were exhibited in the last section.

3.1 Oxidation test

During the experimental workpieces, measured the weights of the specimens before and after putting the specimen in the furnace with a five-digit weighting machine. It was converted to mass gain which weight change divided by surface area of the specimen. Figure 1 shows mass gain in mg.cm^{-2} as a function of time for both stainless steel samples during the oxidation test in O_2-5%H_2O at 800 °C. We found that the mass gain of the high Mn stainless steel sample has values lower than zero and begins at 4 h. It means that spallation behaviors of the thermal oxide growth occur on the surface of the sample. In contrast, the mass gain of low Mn steel rises with time. The result provides that the Mn content in metal substrates has an impact on the formation of thermal oxide.

3.2 Volatilization rates

For the volatile species phase of the thermal oxide growth on stainless, Table 2 shows Cr, Mn and Fe-species volatilization rates of both low and high Mn stainless steel oxidized in O_2-5%H_2O for 96 h at 800 °C. During the oxidation test, the metal volatile phase was

entrapped at the end of the furnace tube in a condenser bottle. The quantitative determination of volatile metal was evaluated by the ICP-OES method. This analytic method can enable the elements in the 0.1 to 50 ppb [18]. The volatilization rate was presented in terms of the mass of volatile metals per surface area and time. It was found that Cr volatilization rates in high Mn stainless steel are 14 times lower than in low Mn stainless steel, while Fe and Mn volatilization rates increase by 10 and 62 times. The dominant volatilization species phases may be hydroxide compounds of Cr Mn and Fe. There were $CrO_2(OH)_2$, $Mn(OH)_2$ and $Fe(OH)_2$, respectively [19].

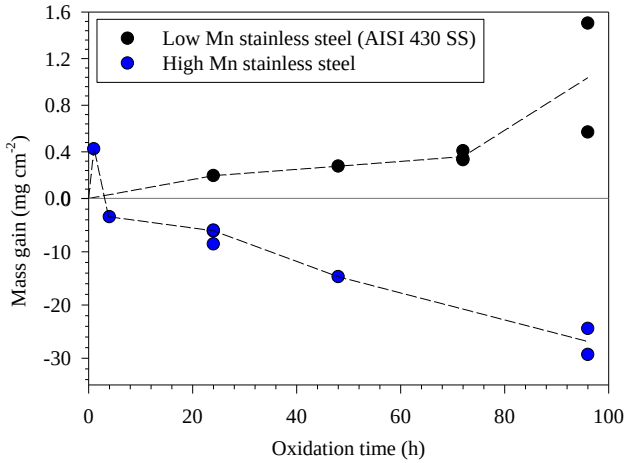

Fig. 1. Mass gain as a function of time of the sample during the oxidation test in O_2 5%H_2O at 800 ºC.

Table 2. Cr, Mn and Fe-species volatilization rates of both low and high Mn stainless steel oxidized in O_2-5%H_2O at 800 ºC for 96 h.

Stainless steel	Volatilization rates (× 10^{-11} g cm^{-2} s^{-1})		
	Cr	Mn	Fe
Low Mn	1.25 ± 0.66	0.08 ± 0.03	1.34 ± 0.48
High Mn	0.09 ± 0.01	4.96 ± 1.52	13.66 ± 6.67

3.3 SEM and EDS

Cross-sectional SEM images and EDS mapping results of the oxidized low Mn stainless steel after the test in O_2-5%H_2O at 800 ºC for 96 h is revealed as shown in Figure 2 at 170x magnitude image. It can see that the thermally grown oxides on the stainless-steel substrate have two types. There is a large nodule of oxide and a thin continuous oxide layer. For the EDS mapping, the outer part of nodule oxide consists of Fe and O which is the main element distribution in outward growth nodule oxide. Moreover, Mn, Fe, and O were detected covering the outer part of nodule oxide. The inner part of the nodule oxide has Cr, Fe, and O. It was indicated that this oxide is an inward growth to metal substrates. Nearly the nodule oxide, a thin continuous oxide layer is found. Mn, Cr, and O were obtained in this layer. For high Mn stainless steel 96 h shown in Figure 3, it has a thicker oxide layer composed of Cr, Mn, Fe and O which surface of the oxide is covered by a thin oxide layer of Mn, Fe and O but most of the outer oxide layer consists of Cr and O.

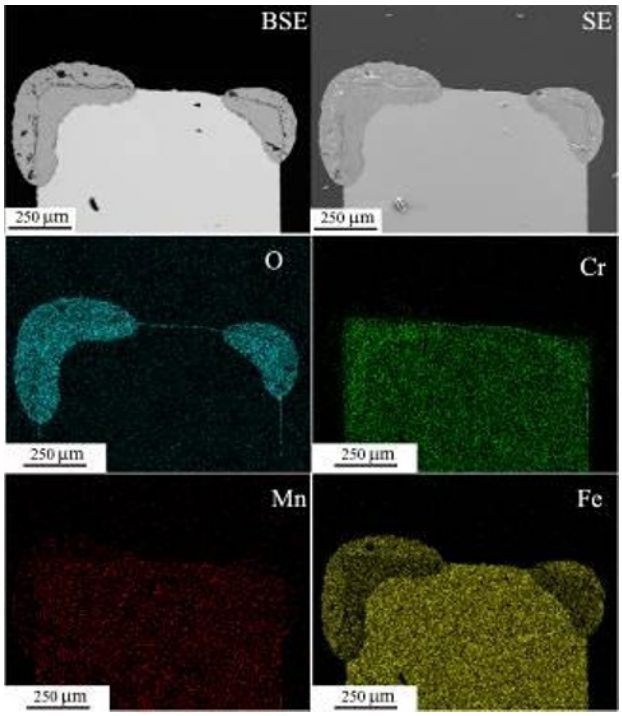

Fig. 2. Cross-sectional micrographs and EDS mapping results of low Mn stainless steel oxidized after 96 h (170x magnitude image).

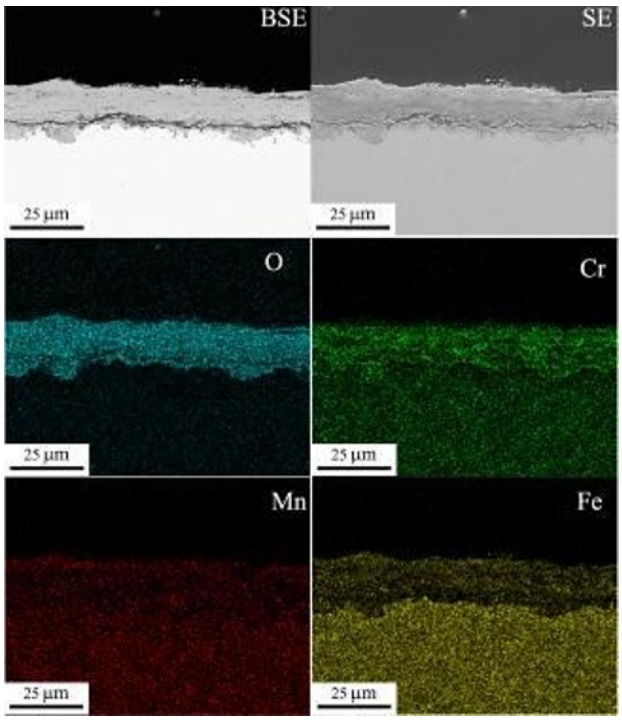

Fig. 3. Cross-sectional micrographs and EDS mapping results of high Mn stainless steel oxidized after 96 h (1,000x magnitude image).

3.4 XRD phase identification

To identify the oxide phases formed after the test, the X-ray diffraction technique was applied to the samples. Figure 4 shows XRD pattern of the oxidized low Mn stainless steel in O_2-5%H_2O at 800 ºC for 96 h. The peaks of $MnFe_2O_4$ (ICDD 00-010-0319), Cr_2O_3 (ICDD 00-002-1362), (Cr, Fe)$_2O_3$ (ICDD 00-002-1357) and Fe_2O_3 (ICDD 00-013-0534) were detected on the surface sample. For the oxidized high Mn stainless steel for 1 h at the same oxidation atmosphere and temperature test, peaks $MnCr_2O_4$ (ICDD 01-075-1614) and $Fe_{0.902}O$ (ICDD 01-086-2316). When increasing the oxidation time to 96 h. The sample has peaks of $MnCr_2O_4$ (ICDD 01-075-1614), Mn_2O_3 (ICD 00-001-1061), Cr_2O_3 (ICDD 00-002-1362) and Fe_3O_4 (ICDD 01-074-0748).

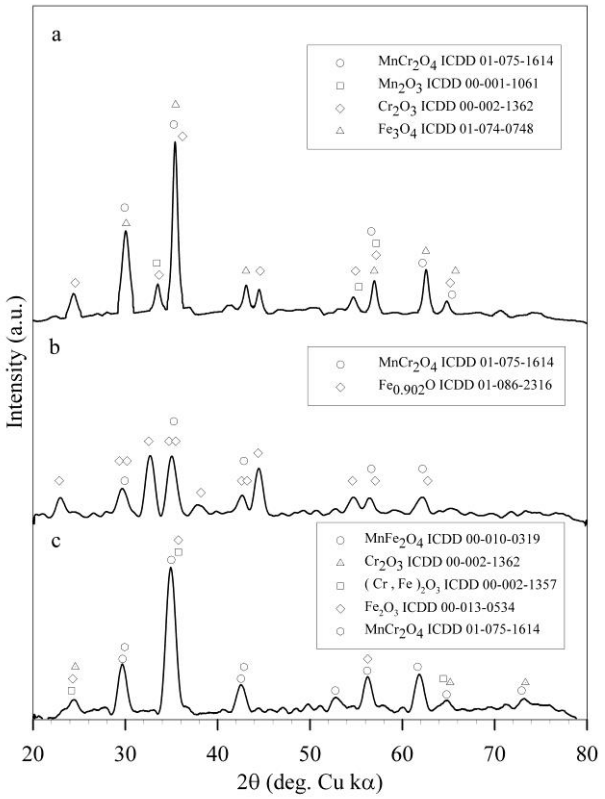

Fig. 4. XRD patterns of high Mn stainless steel oxidized in O_2-5%H_2O at 800 ºC for 96 h (a), 1 h (b) and low Mn stainless steel for 96 h (c)

Figure 5 shows the behavior of oxide growth on low Mn stainless steel. The nodule oxide was formed at an angle on the sample. This nodule occurs because of the direction of the gas flow, the angle was turbulent. Nevertheless, the thin oxide layer beside the nodule was covered by Cr_2O_3 and $MnCr_2O_4$. It is close to the SEM-EDS mapping and XRD results. That is why Cr is highly volatile shown in Table 2. According to Asteman *et. al.* [8] found that the nodule oxide formed (Breakaway oxidation) on 304L stainless steel at 500-800 ºC in O_2-40%H_2O atmospheres as a result of the flow rate. It was obtained from (Cr,Fe)$_2O_3$ and Fe_2O_3 oxide formation. In this case, the results were similar.

From the results of high Mn stainless steel, it can be inferred that the thermal oxide growth was shown in Figure 6. At the initial time, $MnCr_2O_4$ covering FeO was fabricated by Cr and Mn reacting with O. After that $MnCr_2O_4$ and FeO interdiffusion to create the Mn-Cr-Fe oxide. In the long term, Mn and Fe diffuse through the Mn-Cr-Fe oxide to form (Mn,Fe)$_2O_3$ or (Mn,Fe)$_3O_4$ on the top surface. This phase contributes to the volatile phases of Mn and Fe. It related to volatilization rate results, which are measured. When the sample was cooled down from high temperatures to room temperature. Spallation can occur. Moreover, the results were closed to A.L. Marasco and D.J. Young [20]. They found that the high Mn element in stainless steel oxidized at 900 ºC at an oxygen partial pressure of 26.7 kPa, which makes bixbyite-(Mn, Fe)$_2O_3$-and α -Fe_2O_3 oxides and increases the high oxidation rate, then spallation occurs.

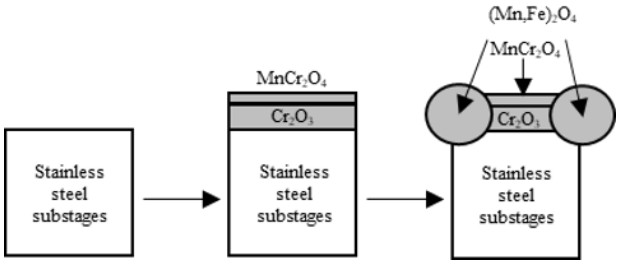

Fig. 5. Schematic sketch behavior of oxide growth on low Mn stainless steel.

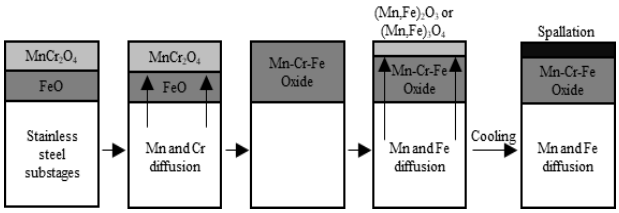

Fig. 6. Schematic sketch behavior of oxide growth on high Mn stainless steel.

4 Conclusion

In the present work, stainless steel with high manganese content (Fe-15.32 wt.% Cr-8.94 wt.% Mn) and low manganese content as AISI 430 stainless steel (Fe-16.41 wt.% Cr-0.79 wt.% Mn) were oxidized in O_2-5%H_2O atmospheres at 800 ºC for 1 h up to 96 h. The summary was described as follows.

1) Manganese in stainless steel induces spallation of oxide after oxidization in O_2-5%H_2O at 800 ºC as a result of nodule oxide formation.
2) Cr volatilization rates in high Mn stainless steel are lower than the other by a factor of 14, while Fe and Mn volatilization rates increase by 10 and 62 times, respectively. It may be possible that Mn-Fe oxide formed at the outer layer.

As a recommendation, the selection of stainless steel for industrial Mn concentration should be suitable to reduce Cr loss and avoid spallation of the oxide scale.

Acknowledgements

The authors acknowledge the financial support from National Science, Research and Innovation Fund (NSRF) and King Mongkut's University of Technology North Bangkok (Contract no. KMUTNB-FF-66-22).

References

1. S. Chandra-Ambhorn, T. Thublaor, C. Pascal, Thermodynamics and kinetics of the high temperature oxidation of stainless steels, Solid State Phenomena, **300**, (2020): 1-24
2. R. Peraldi, B.A. Pint, Effect of Cr and Ni contents on the oxidation behavior of ferritic and austenitic model alloys in air with water vapor, Oxidation of metals, **61**, (2004): 463-483
3. J. Ehlers, D.J. Young, E.J. Smaardijk, A.K. Tyagi, H. J. Penkalla, L. Singheiser, W.J. Quadakkers, Enhanced oxidation of the 9% Cr steel P91 in water vapour containing environments, Corrosion science, **48**, (2006): 3428-3454
4. D.B. Wei, J.X. Huang, A.W. Zhang, Z.Y. Jiang, A.K. Tieu, X. Shi, S.H. Jiao, X.Y. Qu, Study on the oxidation of stainless steels 304 and 304L in humid air and the friction during hot rolling, Wear, **267** (2009): 1741-1745
5. L. Intiso, L.G. Johansson, J.E. Svensson, M. Halvarsson, Oxidation of Sanicro 25 (42Fe22Cr25NiWCuNbN) in O_2 and O_2+H_2O environments at 600-750 ^oC, Oxidation of metals, **83**, (2015): 367-391
6. G. Li, Y. Gou, J. Qiao, W. Sun, Z. Wang, K. Sun, Recent progress of tubular solid oxide fuel cell: From materials to applications, Journal of power sources, **477** (2020): 228693
7. W. Wongpromrat, H. Thaikan, W. Chandra-ambhorn, S. Chandra-ambhorn, Chromium vaporisation from AISI 441 stainless steel oxidised in humidified oxygen, Oxidation of metals, **79**, (2013): 529-540
8. H. Asteman, J.E. Svensson, L.G. Johansson, Evidence for chromium evaporation influencing the oxidation of 304L: the effect of temperature and flow rate, Oxidation of metals, **57**, (2002): 193-216
9. M. Kemp, A. van Bennekom, F.P.A. Robinson, Evaluation of the corrosion and mechanical properties of a range of experimental Cr-Mn stainless steels, Structural Materials: Properties, Microstructure and Processing, **199**, (1995): 183-194
10. R.L. Klueh, P.J. Maziasz, E.H. Lee, Manganese as an austenite stabilizer in Fe-Cr-Mn-C steels, Structural Materials: Properties, Microstructure and Processing, **102**, (1988): 115-124
11. F.H. Stott, G.C. Wood, J. Stringer, The influence of alloying elements on the development and maintenance of protective scales, Oxidation of metals, **44**, (1995): 113-145
12. S.N. Basu, G.J. Yurek, Effect of alloy grain size and silicon content on the oxidation of austenitic Fe-Cr-Ni-Mn-Si alloys in pure O_2, Oxidation of metals, **36**, (1991): 281-315
13. D.L. Douglass, J.S. Armijo, The effect of silicon and manganese on the oxidation mechanism of Ni-20 Cr, Oxidation of metals, **2**, (1970): 207-231
14. D.L. Douglass, J.S. Armijo, The influence of manganese and silicon on the oxidation behavior of Co-20Cr, Oxidation of metals, **3**, (1971): 185-202
15. G.N. Irving, J. Stringer, D.P. Whittle, Effect of the possible fcc stabilizers Mn, Fe, and Ni on the high-temperature oxidation of Co-Cr alloys, Oxidation of metals, **8**, (1974): 393-407
16. H. Falk-Windisch, J.E. Svensson, J. Froitzheim, The effect of temperature on chromium vaporization and oxide scale growth on interconnect steels for Solid Oxide Fuel Cells, Journal of power sources, **287**, (2015): 25-35
17. Barin I. Platzki G. *Thermochemical data of pure substances* (Weinheim: VCh, 1989)
18. McMahon G. *Analytical instrumentation: a guide to laboratory, portable and miniaturized instruments* (John Wiley & Sons, 2008)
19. D.L. Myers, N.S. Jacobson, C.W. Bauschlicher, E.J. Opila, Thermochemistry of volatile metal hydroxides and oxyhydroxides at elevated temperatures. Journal of Materials Research, **34**, (2019): 394-407
20. A.L. Marasco, D.J. Young, The oxidation of Iron-Chromium-Manganese alloys at 900 ^oC, Oxidation of metals, **36**, (1991): 157-174